

BBA 71696

**A MODEL FOR THE REACTION PATHWAYS OF THE  $K^+$ -DEPENDENT PHOSPHATASE ACTIVITY OF THE  $(Na^+ + K^+)$ -DEPENDENT ATPase**

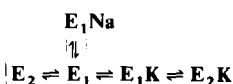
JOSEPH D. ROBINSON, GRACE M. LEVINE and LISA J. ROBINSON

*Department of Pharmacology, State University of New York, Upstate Medical Center, Syracuse, NY 13210 (U.S.A.)*

(Received December 17th, 1982)

*Key words:  $(Na^+ + K^+)$ -ATPase;  $K^+$  dependence; Phosphatase activity; Conformational change; Kinetics*

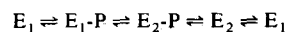
$(Na^+ + K^+)$ -dependent ATPase preparations from rat brain, dog kidney, and human red blood cells also catalyze a  $K^+$ -dependent phosphatase reaction.  $K^+$  activation and  $Na^+$  inhibition of this reaction are described quantitatively by a model featuring isomerization between  $E_1$  and  $E_2$  enzyme conformations with activity proportional to  $E_2K$  concentration:



Differences between the three preparations in  $K_{0.5}$  for  $K^+$  activation can then be accounted for by differences in equilibria between  $E_1K$  and  $E_2K$  with dissociation constants identical. Similarly, reductions in  $K_{0.5}$  produced by dimethyl sulfoxide are attributable to shifts in equilibria toward  $E_2$  conformations.  $Na^+$  stimulation of  $K^+$ -dependent phosphatase activity of brain and red blood cell preparations, demonstrable with KCl under 1 mM, can be accounted for by including a supplementary pathway proportional to  $E_1Na$  but dependent also on  $K^+$  activation through high-affinity sites. With inside-out red blood cell vesicles,  $K^+$  activation in the absence of  $Na^+$  is mediated through sites oriented toward the cytoplasm, while in the presence of  $Na^+$  high-affinity  $K^+$ -sites are oriented extracellularly, as are those of the  $(Na^+ + K^+)$ -dependent ATPase reaction. Dimethyl sulfoxide accentuated  $Na^+$ -stimulated  $K^+$ -dependent phosphatase activity in all three preparations, attributable to shifts from the  $E_1P$  to  $E_2P$  conformation, with the latter bearing the high-affinity, extracellularly oriented  $K^+$ -sites of the  $Na^+$ -stimulated pathway.

**Introduction**

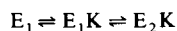
The reaction sequence of the  $(Na^+ + K^+)$ -dependent ATPase may be condensed into four steps



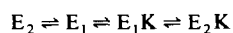
representing two chemical changes, enzyme phosphorylation by ATP to form  $E_1\text{-P}$  and hydrolysis of the acyl phosphate to form  $E_2$ , separated by two isomerizations between  $E_1$  and  $E_2$  conformational forms, probably linked to the cation transport role of this enzyme [1–3]. Early enzymatic studies distinguished between ADP- and  $K^+$ -sensitive phosphoenzymes, representing the  $E_1\text{-P}$  and  $E_2\text{-P}$  conformations [4,5]; subsequent studies on enzyme fluorescence [6] and tryptic digestion [7] revealed  $Na^+$ - and  $K^+$ -selected forms, equated to  $E_1$  and  $E_2$ , respectively.

Abbreviations:  $K^+$ -phosphatase,  $K^+$ -dependent *p*-nitrophenyl phosphatase; Me<sub>2</sub>SO, dimethyl sulfoxide;  $(Na^+ + K^+)$ -ATPase,  $(Na^+ + K^+)$ -dependent adenosine triphosphatase.

The enzyme also catalyzes a  $K^+$ -dependent phosphatase reaction presumably involving  $E_2$  conformational forms and reflecting the hydrolytic steps of the overall ATPase reaction. Recent experiments on the phosphatase activity in conjunction with tryptic digestion of the enzyme [8] reveal a discrepancy between earlier formulations for the conformational stages involved in fluorescence and tryptic digestion studies [9,10] and measurements of enzyme activity. Thus, the previous scheme



could not account for divergence between the  $K_{0.5}$  for  $K^+$  affecting fluorescence changes and that for activating  $K^+$ -phosphatase activity, and required expansion of the equilibria to:



In this amended scheme, tryptic digestion and fluorescence changes would represent the ratio of total  $E_1$  and  $E_2$  conformations, whereas  $K^+$ -phosphatase activity would be proportional only to  $E_2K$  [8]. This discrepancy thus emphasizes the necessity for considering measurements of enzymatic activity when interpreting measurements of conformational states.

The experiments described here were designed to explore these issues further, in terms of the requisite conformational forms involved in the  $K^+$ -phosphatase reaction as a function of the activating ligands  $K^+$ ,  $Mg^{2+}$  and substrate, together with an examination of the effects of reagents that alter the isomerization between conformations, such as  $Mn^{2+}$  and dimethyl sulfoxide. In addition, the experiments deal with the peculiar stimulation by  $Na^+$  in the presence of low concentrations of  $K^+$ , with attention to the localization on the enzyme faces of the pertinent cation sites. For these purposes, the parameters of the model were evaluated quantitatively for enzymes from three sources: rat brain, dog kidney, and human red blood cells. Although the enzymatic responses differed quantitatively (for example,  $K_{0.5}$  for  $K^+$ ) and qualitatively (for example, stimulation versus inhibition by  $Na^+$ ), enzymes from these sources could be fitted to the same model with relatively small changes in parameters.

## Methods and Materials

The enzyme was prepared from rat brain as previously described [11] and from dog kidney according to Jørgensen [12]. Permeable red blood cell ghosts were made by hypotonic lysis of human cells [13] followed by two freeze-thaw cycles. Inside-out red blood cell vesicles were prepared as previously described [13,14]. To adjust the intravesicular contents the vesicles, originally equilibrated with 3 mM Tris adjusted to pH 7.4 with glycylglycine, were incubated for 2 days at 0–4°C with appropriate media [14].

$K^+$ -dependent phosphatase activity was measured in terms of the liberation of *p*-nitrophenol during incubations at 37°C using *p*-nitrophenyl phosphate as substrate, as previously described [15]. For experiments with brain and kidney enzyme preparations and permeable red blood cell ghosts, the standard incubation medium contained 30 mM histidine-HCl adjusted to pH 7.8 with Tris, 3 mM *p*-nitrophenyl phosphate (as the Tris salt), 3 mM  $MgCl_2$  and 10 mM KCl.  $K^+$ -independent activity, when present, was measured by parallel incubations in media omitting KCl and including 0.3 mM ouabain, and such activity was subtracted from total activity in the presence of KCl to give  $K^+$ -dependent activity. For experiments with inside-out vesicles, 3 mM Tris adjusted to pH 7.4 with glycylglycine was used as buffer, with osmolarity maintained by addition of choline chloride [15].  $K^+$ -independent activity was measured by addition of 20  $\mu$ M strophanthidin.

Data presented are means of four or more experiments, each performed in duplicate to quadruplicate, and are listed  $\pm$  S.E. where pertinent.

*p*-Nitrophenyl phosphate, ouabain and strophanthidin were obtained from Sigma Chemical Corp.

## Results

### *Activation of the brain enzyme by $K^+$ , $Na^+$ and dimethyl sulfoxide*

For the  $K^+$ -phosphatase reaction catalyzed by the rat brain ( $Na^+ + K^+$ )-ATPase enzyme, activation by KCl followed a sigmoidal activator-velocity pattern, with double-reciprocal plots concave

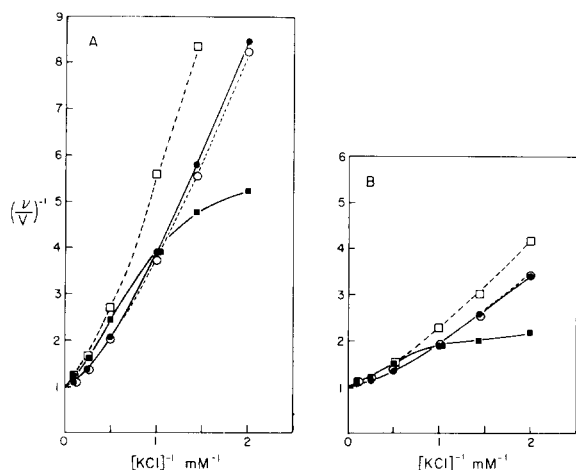


Fig. 1. Effects of KCl, NaCl and Me<sub>2</sub>SO on K<sup>+</sup>-phosphatase activity of the rat brain enzyme. Panel A shows activity measured in the standard medium (see Methods and Materials) modified to contain the KCl concentrations indicated, in the absence (●) or presence (■) of 10 mM NaCl; data are presented in double-reciprocal form. Panel B shows corresponding experiments in the presence of 10% (v/v) Me<sub>2</sub>SO; the maximal velocity in the presence of Me<sub>2</sub>SO averaged 1.9-times that in its absence. In addition, calculated values for the velocities over pathway A, using the parameters in Table I for the model in Fig. 2, are shown in the absence (○) or presence (□) of 10 mM NaCl.

upward (Fig. 1A) and Hill plots having  $n > 1$ , as previously described [15]. Addition of 10% (v/v) Me<sub>2</sub>SO to the incubation medium increased the maximal velocity 2-fold, and decreased the  $K_{0.5}$  for K<sup>+</sup> from 2.1 to 0.95 mM (Fig. 1B), as previously described [16].

The effects of adding NaCl to the reaction mixture were, however, more complex. Although at higher KCl concentrations (over 1 mM) adding 10 mM NaCl inhibited activity, at lower concentrations NaCl stimulated, producing a phase of the double-reciprocal plot of KCl concentration vs. velocity concave downward (Fig. 1A), as previously described [15,17,18]. A similar response to NaCl also occurred in the presence of Me<sub>2</sub>SO (Fig. 1B).

Activation by KCl can be fitted to the model shown in Fig. 2. This formulation was previously proposed to account for the differential responses of K<sup>+</sup>-phosphatase activity and of fluorescence

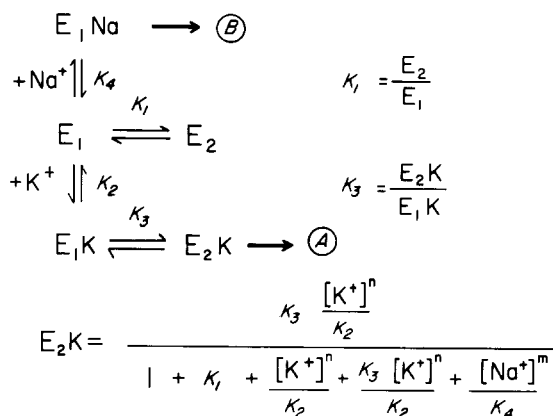


Fig. 2. Model for K<sup>+</sup> and Na<sup>+</sup> effects on K<sup>+</sup>-phosphatase activity. The four constants describe equilibria between the conformational states ( $K_1$  and  $K_3$ ) and the dissociation of K<sup>+</sup> ( $K_2$ ) and Na<sup>+</sup> ( $K_4$ ), with the relative concentration of E<sub>2</sub>K expressed as a function of these constants, the concentrations of the cations, and the Hill coefficients for cooperativity in the K<sup>+</sup> ( $n$ ) and Na<sup>+</sup> ( $m$ ) sites. Activity in the absence of Na<sup>+</sup> is considered to be proportional to E<sub>2</sub>K (pathway A), while in the presence of Na<sup>+</sup> it is the sum of pathway A plus pathway B, the latter proportional to E<sub>1</sub>Na.

changes of the enzyme to KCl concentration [8], with K<sup>+</sup>-phosphatase activity proportional to the E<sub>2</sub>K concentration and fluorescence changes to the sum of E<sub>2</sub> and E<sub>2</sub>K concentrations. Although an optimal selection of parameters was not attempted, a good fit to the data for K<sup>+</sup> activation in Fig. 1, as shown by the open circles and dashed lines, was achieved with the values shown in Table I. The effect of Me<sub>2</sub>SO on K<sup>+</sup> activation is attributed to increases in  $K_1$  and  $K_3$ , relating to the isomerization between E<sub>1</sub> and E<sub>2</sub> forms, without change in  $K_2$ , the dissociation constant for K<sup>+</sup>-binding to E<sub>1</sub> (Fig. 2; Table I).

Inhibition by NaCl also can be fitted by this model with velocity proportional to E<sub>2</sub>K (pathway A), as shown by the open squares and dashed lines of Figs. 1A and B, although the data are approximated at only the three higher KCl concentrations. Again, effects of Me<sub>2</sub>SO are attributed to changes in  $K_1$  and  $K_3$  and not in the dissociation constants for either cation,  $K_2$  and  $K_4$  (Table I). On the other hand, stimulation by NaCl at low KCl concentrations (Figs. 1A,B) clearly cannot be related to the concentration of E<sub>2</sub>K alone.

TABLE I

VALUES OF CONSTANTS FOR FIGS. 1, 3, 4 AND 8

These constants were used in the equation of Fig. 2 to calculate the dashed lines of Figs. 1, 3 and 8 for velocity over pathway A, with maximal velocity at infinite KCl concentration defined as 1.0. For Fig. 4 the dashed lines represent the calculated total velocities over pathways A and B: the sums of velocity over pathway A, as above, plus velocity over pathway B, obtained by multiplying the concentration of  $E_1Na$  by  $b$ , an empirical factor reflecting maximal velocity over pathway B relative to that over A as well as the effective saturation of  $K^+$ -sites in pathway B. For brain and red blood cell enzymes values for  $b$  were estimated similarly, except that only a single concentration of NaCl, 10 mM (Figs. 1 and 8), was used for calculation: thus  $b[E_1Na]$  was set equal to observed velocity (Figs. 1 and 8) minus calculated velocity over pathway A in the presence of 10 mM NaCl.

Constant	Brain enzyme		Kidney enzyme		Red cell enzyme
	– Me <sub>2</sub> SO	+ Me <sub>2</sub> SO	– Me <sub>2</sub> SO	+ Me <sub>2</sub> SO	– Me <sub>2</sub> SO
$K_1$	0.5	2.0	0.5	2.0	0.5
$K_2$ (mM)	11.1	11.1	11.1	11.1	11.1
$K_3$	5.0	35.0	15.0	45.0	5.5
$K_4$ (mM)	12.5	12.5	12.5	12.5	12.5
$n$	1.4	1.35	1.5	1.4	1.25
$m$	1.1	1.1	1.4	1.3	1.1
$b$ ( $K^+ = 0.7$ mM)	0.44	1.04	–	–	0.26
( $K^+ = 0.5$ mM)	0.26	1.15	0.06	0.42	0.25
( $K^+ = 0.3$ mM)	–	–	0.05	0.35	–

#### Activation of the kidney enzyme by $K^+$ , $Na^+$ and dimethyl sulfoxide

For the  $K^+$ -phosphatase reaction catalyzed by the dog kidney enzyme, activation again followed a sigmoidal activator-velocity pattern, with double-reciprocal plots concave upward (Fig. 3A) and Hill plots having  $n > 1$ . Me<sub>2</sub>SO again stimulated, but with only a 1.5-fold increase in maximal velocity, as well as a lesser decrease in  $K_{0.5}$  for  $K^+$ , from 1.1 to 0.7 mM (Figs. 3A,B). These responses to  $K^+$  and Me<sub>2</sub>SO can be fitted (Figs. 3A,B: open circles) to the model in Fig. 2, with the lower  $K_{0.5}$  for  $K^+$  of the kidney enzyme represented by a change in the isomerization constant,  $K_3$ , rather than in the dissociation constant,  $K_2$ , and with the lesser effects of Me<sub>2</sub>SO represented by a smaller increase in  $K_3$  (Table I).

Unlike the brain enzyme, the kidney enzyme was not obviously stimulated by NaCl at low KCl concentration, although again a phase of the plot is concave downward (Fig. 3A). Direct comparison is complicated by the difference in  $K_{0.5}$  for  $K^+$ , but at a concentration of KCl sufficient to produce 20% of maximal velocity adding 10 mM NaCl stimulated the brain enzyme 10% (Fig. 1A) but inhibited the kidney enzyme 37% (Fig. 3A). In

the presence of Me<sub>2</sub>SO, however, stimulation by NaCl did become apparent (Fig. 3B), and at a concentration of KCl sufficient to produce 20% of maximal velocity, adding 10 mM NaCl then stimulated the kidney enzyme 18%.

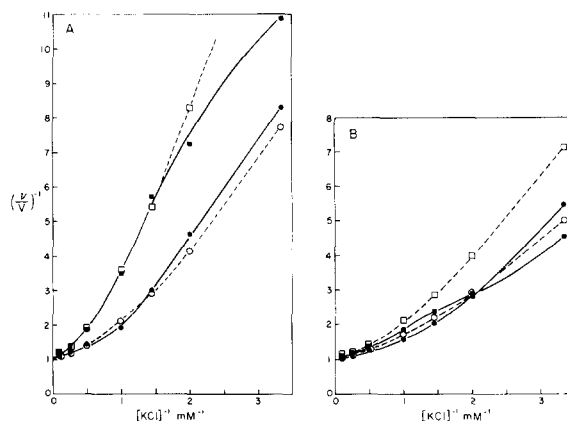


Fig. 3. Effects of KCl, NaCl and Me<sub>2</sub>SO on  $K^+$ -phosphatase activity of the dog kidney enzyme. Experiments were performed and the data are presented as in Fig. 1 (●, no NaCl; ■, 10 mM NaCl) from studies in the absence (panel A) or presence (panel B) of Me<sub>2</sub>SO, together with the calculated values (○, □). The maximal velocity in the presence of Me<sub>2</sub>SO averaged 1.5-times that in its absence.

The model again describes inhibition by NaCl at high KCl concentrations as shown by the open squares and dashed lines of Figs. 3A and B, although, as in the case of the brain enzyme, actual velocities with low KCl concentrations were greater than calculated velocities.

With either 0.3 or 0.5 mM KCl activity progressively fell as NaCl was added in the range 0.3 to 30 mM (Figs. 4A,B). In the presence of  $\text{Me}_2\text{SO}$ , however, velocity first increased somewhat but then fell with NaCl concentrations above 10 mM. As previously proposed [17,18], stimulation by  $\text{Na}^+$  at low  $\text{K}^+$  concentrations may represent the availability of an alternative enzymatic pathway requiring both  $\text{Na}^+$  and  $\text{K}^+$  and having a higher affinity for  $\text{K}^+$ . The model in Fig. 2 can accommodate this proposal by considering the total observed activity to represent the sum of the activity over pathway A, proportional to the concentration of  $\text{E}_2\text{K}$ , plus that over pathway B, proportional to the concentration of  $\text{E}_1\text{Na}$ . To sum the activities, a factor,  $b$ , is multiplied by the  $\text{E}_1\text{Na}$  concentration, reflecting the maximal velocity of pathway B relative to A and the effective saturation of pathway B by  $\text{K}^+$  (thus  $b$  is a function of KCl concentration). With these assumptions, the dashed lines of Figs. 4A and B are generated from the parameters of

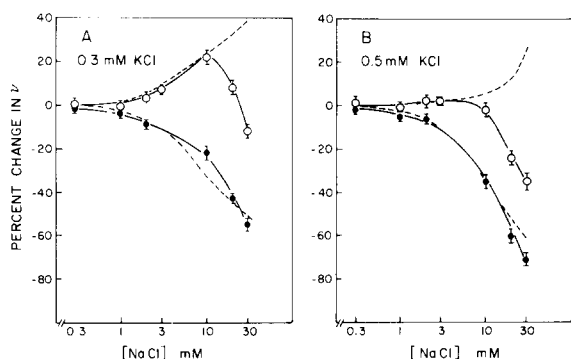


Fig. 4. Effects of NaCl on  $\text{K}^+$ -phosphatase activity of the dog kidney enzyme. Panel A shows activity in the standard medium modified to contain 0.3 mM KCl and the concentrations of NaCl shown, in the absence (●) or presence (○) of  $\text{Me}_2\text{SO}$ . Panel B shows corresponding values for experiments with 0.5 mM KCl. In addition, calculated values for the velocities are shown as the dashed lines, using the parameters in Table I for the model in Fig. 2; changes in velocity are calculated by equating total velocity to the sum of  $\text{E}_2\text{K}$  plus  $b$  times  $\text{E}_1\text{Na}$  for the successive concentrations of NaCl.

Table I by including the factors for pathway B shown.

#### Effects of $\text{MgCl}_2$ , $\text{MnCl}_2$ and nitrophenyl phosphate

With 0.3 mM KCl stimulation by NaCl may be shown even in the absence of  $\text{Me}_2\text{SO}$  by increasing the  $\text{MgCl}_2$  concentration from 3 mM to 9 mM (Fig. 5). These data were not fitted quantitatively to the model because further complexities are introduced. Raising the  $\text{MgCl}_2$  concentration itself reduced activity, more so at lower KCl concentrations, suggesting competition for the  $\text{K}^+$ -sites, and with 0.3 mM KCl, substituting 9 mM  $\text{MgCl}_2$  for 3 mM  $\text{MgCl}_2$ , activity was inhibited  $32 \pm 2\%$ . As shown, with 3 mM  $\text{MgCl}_2$  and 0.3 mM KCl adding 30 mM NaCl reduced activity by  $55 \pm 4\%$  (Fig. 4A) whereas with 9 mM  $\text{MgCl}_2$  and 0.3 mM KCl adding 30 mM NaCl increased activity by  $26 \pm 3\%$  (Fig. 5). Consequently, relative activities with 0.3 mM KCl were 1.0 with 3 mM  $\text{MgCl}_2$  and no NaCl vs. 0.45 with 30 mM NaCl, and 0.68 with 9 mM  $\text{MgCl}_2$  and no NaCl vs. 0.86 with 30 mM NaCl. Thus, although separately  $\text{Mg}^{2+}$  and  $\text{Na}^+$

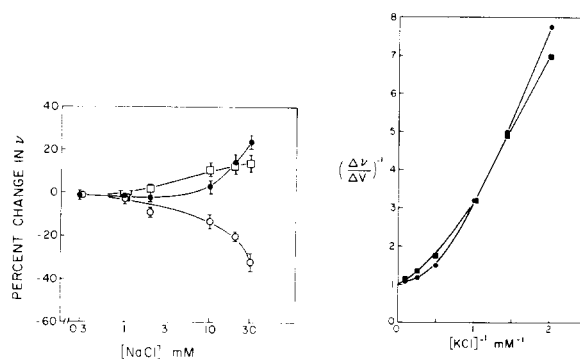


Fig. 5. Effects of  $\text{MgCl}_2$ ,  $\text{MnCl}_2$  and nitrophenyl phosphate on  $\text{K}^+$ -phosphatase activity of the dog kidney enzyme. Activity was measured in the standard medium modified to contain the concentrations of NaCl indicated and with 9 mM nitrophenyl phosphate (○) or 9 mM  $\text{MgCl}_2$  (●) in the presence of 0.3 mM KCl, or with 3 mM  $\text{MnCl}_2$  substituted for  $\text{MgCl}_2$  in the presence of 0.5 mM KCl (□).

Fig. 6. Effect of  $\text{MnCl}_2$  on activation of the dog kidney enzyme by KCl and NaCl. Experiments were performed as in Fig. 3A except that 3 mM  $\text{MnCl}_2$  was substituted for 3 mM  $\text{MgCl}_2$ ; data are presented as the increment in ouabain-inhibitable activity due to KCl, since significant  $\text{K}^+$ -independent ouabain-inhibitable activity is demonstrable in the presence of  $\text{MnCl}_2$  [19]. ●, no NaCl; ■, 10 mM NaCl.

inhibited, together inhibition was less than with each alone.

Analogously, substituting 3 mM  $\text{MnCl}_2$  for  $\text{MgCl}_2$  permitted stimulation by NaCl even in the presence of 0.5 mM KCl, again in the absence of  $\text{Me}_2\text{SO}$  (Fig. 5). With 3 mM  $\text{MnCl}_2$  stimulation by NaCl is demonstrable at KCl concentrations sufficient to produce 20% of the maximally stimulated velocity and lower (Fig. 6); these experiments with  $\text{MnCl}_2$  also may not be readily fitted to the model since there is appreciable ouabain-inhibitable phosphatase activity with  $\text{MnCl}_2$  even in the absence of added KCl, suggesting a catalytically active  $\text{E}_2\text{Mn}$  enzyme form [19].

Increasing the substrate concentration from 3 to 9 mM did not produce overt stimulation by NaCl, but the inhibition was less: 26% with 9 mM nitrophenyl phosphate compared to 55% with 3 mM (Figs. 4A, 5).

As the KCl concentration was decreased, the apparent  $K_m$  for nitrophenyl phosphate decreased (Fig. 7A; Table II), as previously described for the brain enzyme [15]. Correspondingly, as the nitrophenyl phosphate concentration was decreased the  $K_{0.5}$  for KCl decreased, from 1.3 mM with 9 mM nitrophenyl phosphate to 0.8 mM with

TABLE II

EFFECT OF  $\text{K}^+$  AND  $\text{Na}^+$  ON  $K_m$  FOR NITROPHENYL PHOSPHATE AND  $K_i$  FOR  $\text{P}_i$

Values for the  $K_m$  for nitrophenyl phosphate, measured in the standard medium (see Methods and Materials) modified to contain the monovalent cations shown, were determined for kidney enzyme from double-reciprocal plots (Fig. 7). Similarly, the values for the  $K_i$  for  $\text{P}_i$  were determined from Dixon plots.

Cations	$K_m$ for substrate (mM)		$K_i$ for $\text{P}_i$ (mM)	
	– $\text{Me}_2\text{SO}$	+ $\text{Me}_2\text{SO}$	– $\text{Me}_2\text{SO}$	– $\text{Me}_2\text{SO}$
KCl, 10 mM	2.93	2.03	1.35	0.70
KCl, 0.5 mM	1.18	1.04	0.52	0.40
+ NaCl, 10 mM	1.54	1.40	1.39	0.83
KCl, 0.3 mM	0.69	0.60		
+ NaCl, 10 mM	1.24	1.12		

1 mM (data not presented), again as with the brain enzyme [15]. In accord with the effect of nitrophenyl phosphate concentration on inhibition by NaCl (Fig. 5), addition of NaCl increased the apparent  $K_m$  for nitrophenyl phosphate (Fig. 7A; Table II). In the presence of  $\text{Me}_2\text{SO}$  similar responses occurred, although values for the  $K_m$  were in all cases somewhat lower (Fig. 7B; Table II).

$\text{P}_i$  is a competitive inhibitor toward nitrophenyl phosphate [20], and the  $K_i$  decreased when the KCl concentration was reduced to 0.5 mM and increased when NaCl was added (Table II). In the presence of  $\text{Me}_2\text{SO}$ , the  $K_i$  values changed similarly, but in all cases were somewhat lower (Table II).

#### Activation of the red blood cell enzyme by $\text{K}^+$ and $\text{Na}^+$

With permeable human red blood ghosts (allowing free access to both faces of the enzyme) the responses to  $\text{K}^+$  alone and to  $\text{Na}^+$  plus  $\text{K}^+$  (Fig. 8) were similar to those of the brain enzyme (Fig. 1). As with the brain enzyme, stimulation by  $\text{Na}^+$  was apparent at a KCl concentration sufficient to produce 20% of maximal velocity. Moreover, activation by  $\text{K}^+$  and inhibition by  $\text{Na}^+$  (at higher KCl concentrations) could again be fitted in terms of pathway A of the model using parameters near those for the brain enzyme (Table I).

To determine whether the proposed activation

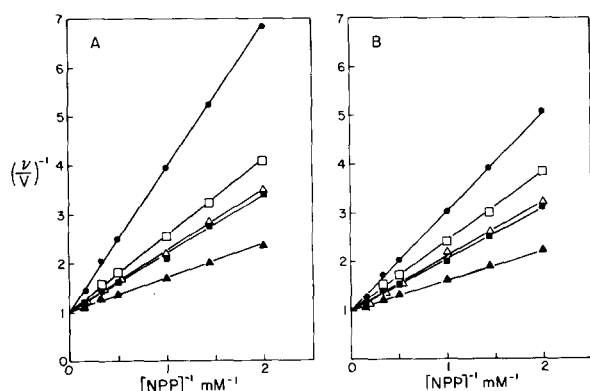


Fig. 7. Effect of KCl, NaCl and  $\text{Me}_2\text{SO}$  on substrate kinetics of the dog kidney enzyme. Panel A shows activity measured in the standard medium modified to contain the concentrations of nitrophenyl phosphate (NPP) indicated and with 10 mM (●), 0.5 mM (■) or 0.3 mM (▲) KCl alone, or 0.5 mM KCl plus 10 mM NaCl (□) or 0.3 mM KCl plus 10 mM NaCl (Δ). Panel B shows corresponding experiments in the presence of  $\text{Me}_2\text{SO}$ . In all cases the  $\text{MgCl}_2$  concentration was 3 mM. Values for  $K_m$  (Table II) were obtained by a least-squares linear regression for these data.

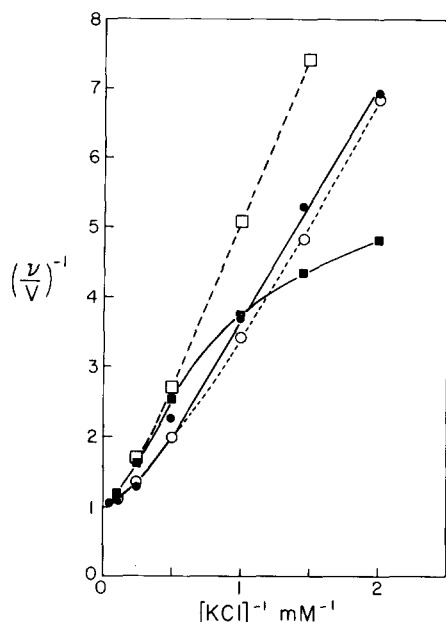


Fig. 8. Effects of KCl and NaCl on  $K^+$ -phosphatase activity of permeable ghosts from human red blood cells. Experiments were performed and data are presented as in Fig. 1 (●, ○, no NaCl; ■, □, 10 mM NaCl).

of pathway B was mediated through  $K^+$ -sites accessible from the cytoplasmic face of the membrane (as is pathway A) or from the extracellular

face (as is the  $(Na^+ + K^+)$ -ATPase), experiments must be performed with enzyme preparations in which 'sidedness' is maintained. Inside-out red blood cell membrane vesicles permit free access of substrate to the cytoplasmic face (now exposed to the medium), with access to the extracellular face (now intravesicular) gained through prior equilibration. Using this preparation  $K^+$ -phosphatase activity in the absence of NaCl was activated only by cytoplasmic KCl, whereas in the presence of cytoplasmic NaCl, extracellular KCl activated (Table III). Moreover, the magnitudes of these agreed well with those from experiments using permeable red blood cell ghosts (Fig. 8).

### Discussion

These studies support a model for the  $K^+$ -phosphatase reaction depicting cation binding to specific sites on the enzyme and isomerization between the  $E_1$  and  $E_2$  conformational states proposed as cyclic steps in the overall  $(Na^+ + K^+)$ -ATPase reaction sequence [3,4]. The model accounts quantitatively for  $K^+$  activation and for inhibition by  $Na^+$  at high  $K^+$  concentrations but stimulation at low  $K^+$  concentrations; it also accounts for variations in  $K_{0.5}$  between enzymes from three sources, for effects of  $Me_2SO$ ,  $Mg^{2+}$

TABLE III

#### SIDEDNESS OF CATION ACTIVATION

The 'extracellular' concentration (intravesicular concentration) was established by equilibration of the inside-out red blood cell vesicles for 2 days at 4°C, as described previously [14]; osmotic balance was maintained by varying the choline chloride concentration. To measure activity, the equilibrated vesicles were diluted into 20 vol. medium to produce the final concentrations shown as 'cytoplasmic'.  $K^+$ -phosphatase activity is expressed relative to that of concurrent determinations of activity with only 10 mM 'cytoplasmic' KCl, defined as 1.00.

'Cytoplasmic' concentrations (mM)		'Extracellular' concentrations (mM)		Relative activity of inside-out red blood cell vesicles
KCl	NaCl	KCl	NaCl	
10	0	0	0	(1.00)
0.5	0	0	0	$0.13 \pm 0.03$
0.5	0	10	0	$0.08 \pm 0.04$
0	0	0.5	0	$-0.01 \pm 0.02$
0.5	0.5	0	10	$0.12 \pm 0.02$
10	10	0	0	$0.92 \pm 0.05$
0.5	10	0	0	$0.09 \pm 0.03$
0.5	10	0.5	0	$0.23 \pm 0.02$
0	0.5	0.5	10	$0.02 \pm 0.04$

and  $\text{Mn}^{2+}$  on the reaction parameters, and for the sidedness of  $\text{K}^+$  activation in the absence and presence of  $\text{Na}^+$ . The model assumes rapid equilibrium for convenience and because steady-state methods are inadequate for first-order isomerizations [21], and can be justified pragmatically by the fit to the data. With six constants, unique evaluations are not possible; nevertheless, plausible values were obtained with  $K_1 < 1$  and  $K_3 > 1$ , in qualitative agreement with fluorescence studies [6], even though the isomerizations invoked appear sensitive to pH, buffer composition and ionic strength [22,23].

The model describes quantitatively activation by  $\text{K}^+$  and inhibition by  $\text{Na}^+$  at high  $\text{K}^+$  concentrations (Figs. 1,3,8). Discrepancies in apparent affinities for  $\text{K}^+$  as activator and  $\text{Na}^+$  as inhibitor between enzymes from three sources are attributed to differences in the isomerization constants ( $K_1$  and  $K_3$ ), reflecting either variations in peptide composition or in enzyme environments, rather than to differences in the respective dissociation constants ( $K_2$  and  $K_4$ ). Relating these constants to reported measurements of the dissociation constants (e.g., Refs. 23–25), however, is difficult not only because of the range of those values but also because they were not measured under substrate,  $\text{MgCl}_2$  and ionic strength conditions used in the assays here.

The ability of  $\text{Me}_2\text{SO}$  to increase the apparent affinity for  $\text{K}^+$  (decrease the  $K_{0.5}$ ) can also be accounted for solely by changes in  $K_1$  and  $K_3$  (Figs. 1, 3; Table I). That  $\text{Me}_2\text{SO}$  favors  $\text{E}_2$  conformations is supported by earlier studies showing it inhibits ADP/ATP exchange dependent on the  $\text{E}_1\text{-P}$  conformation [26], potentiates vanadate binding to  $\text{E}_2\text{K}$  [14], promotes the  $\text{K}^+$  pattern of tryptic digestion [8], and favors the characteristic  $\text{E}_2$  fluorescence changes of the fluoresceine isothiocyanate-labeled enzyme (Steinberg, M. and Robinson, J.D., unpublished observations). The lesser effect of  $\text{Me}_2\text{SO}$  on the  $K_{0.5}$  for  $\text{K}^+$  with kidney enzyme compared to brain enzyme thus may be attributed to the lesser change in  $K_3$  (Table I), since in the absence of  $\text{Me}_2\text{SO}$ ,  $K_3$  for the kidney enzyme is larger than that for brain enzyme.

Stimulation by  $\text{Na}^+$  at low  $\text{K}^+$  concentrations is here attributed to catalysis over an alternative

$\text{Na}^+$ -dependent pathway with high-affinity  $\text{K}^+$ -sites (Fig. 2: pathway B), since  $\text{Na}^+$  alone is an extremely feeble activator [15]. As previously proposed [17,18], this pathway most likely involves  $\text{Na}^+$ -dependent phosphorylation of the enzyme by nitrophenyl phosphate to form  $\text{E}_1\text{-P}$ , followed by isomerization to  $\text{E}_2\text{-P}$  with its high-affinity  $\text{K}^+$ -sites oriented extracellularly, analogous to the  $(\text{Na}^+ + \text{K}^+)\text{-ATPase}$  reaction sequence. An earlier study showed  $\text{Na}^+$ -stimulated, hydroxylamine-sensitive phosphorylation by nitrophenyl phosphate [27], and experiments with inside-out red blood cell vesicles described here show that whereas only cytoplasmic  $\text{K}^+$  activates in the absence of  $\text{Na}^+$ , as first shown by Drapeau and Blostein [28], in the presence of cytoplasmic  $\text{Na}^+$ , extracellular  $\text{K}^+$  activates (Table III). This latter is analogous to activation of the  $\text{K}^+$ -phosphatase reaction by extracellular  $\text{K}^+$  in the presence of cytoplasmic  $\text{Na}^+$  plus ATP [28]. This localization of cation sites also argues against an earlier proposal [29] to account for  $\text{Na}^+$  stimulation. That model invoked 'catalytic' and 'regulatory' sites for the cations, with activity dependent on  $\text{K}^+$  occupying the catalytic site and either  $\text{K}^+$  or  $\text{Na}^+$  occupying the regulatory site. Since maximal activity occurs with only cytoplasmic  $\text{K}^+$  [28] but in the presence of cytoplasmic  $\text{Na}^+$  activity is stimulated by extracellular  $\text{K}^+$  (Table III), the further multiplication of cation sites for that model is required.

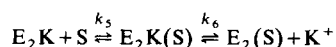
Pathway B is quantitated here only in terms of the empirical parameter,  $b$ , which varies with  $\text{K}^+$  concentration (Table I). However,  $b$  may be expressed in the above mechanism as  $V_B/D$ , where  $V_B$  is the maximal velocity over pathway A, and  $D$  incorporates  $\text{K}^+$  activation and  $\text{Na}^+$  competition in this pathway:  $(K_k[\text{K}^+]^{-1}(1 + [\text{Na}^+]K_{na}^{-1}))^p$  where  $K_k$  and  $K_{na}$  are dissociation constants for, respectively,  $\text{K}^+$  and  $\text{Na}^+$  at the high-affinity sites and  $p$  is the Hill coefficient for the sites. This elaboration of  $b$  obviously can account for inhibition at high  $\text{Na}^+$  concentrations (Fig. 4), as also seen in the  $(\text{Na}^+ + \text{K}^+)\text{-ATPase}$  reaction [30], but evaluation of these four additional parameters did not seem justified by the available data. Furthermore, stimulated hydrolysis over pathway B could be due not merely to hydrolysis of  $\text{E}_2\text{-P}$  but also to the  $\text{K}^+$  bound through the high-affinity sites remaining on the enzyme to activate further hydrolysis.



ysis over pathway A; this later explanation is analogous to a proposal for  $K^+$ -phosphatase stimulation by  $Na^+$  plus ATP [2].

In either case, the model can again account both for stimulation by  $Na^+$  at low  $K^+$  concentrations with brain and red blood cell enzymes and for lack of overt stimulation with kidney enzyme, through differences in isomerization constants  $K_1$  and  $K_3$  and in  $b$  (which also includes within  $V$  an isomerization constant for the  $E_1$ -P to  $E_2$ -P transition). Since  $Me_2SO$  favors  $E_2$  conformations, it may seem strange that it also favors the  $Na^+$  stimulation (Fig. 3) interpreted as dependent on  $E_1Na$ . An obvious mechanism is that  $Me_2SO$  by favoring conversion of  $E_1$ -P to  $E_2$ -P increases availability of high-affinity  $K^+$ -sites. Similarly, stimulation of pathway B by  $Mg^{2+}$  and  $Mn^{2+}$  (Fig. 5) may be attributed to these cations (particularly  $Mn^{2+}$ ) favoring  $E_2$  conformations [31].

The model in Fig. 2, however, does not describe the relationships between apparent  $K_m$  for substrate,  $K_{0.5}$  for  $K^+$ , and  $K_i$  for  $P_i$  (Table II). The reciprocal changes in  $K_m$  and  $K_{0.5}$  may be accounted for by nitrophenyl phosphate and  $K^+$  each binding more tightly to enzyme forms in the absence of the other. Nitrophenyl phosphate, nevertheless, seems to favor  $E_2$  enzyme forms, as indicated by  $Me_2SO$  decreasing the  $K_m$  and by  $Na^+$  increasing it. Moreover,  $P_i$ , which is a competitor toward nitrophenyl phosphate, binds like vanadate to  $E_2$  forms [14]. Consequently, additional enzyme states must be included:



where S refers to nitrophenyl phosphate. These additional constants are compounded within the constants of Table I; nevertheless, the data (Table II) show that both  $K_5$  and  $K_6$  must be greater than 1.  $Me_2SO$  also must not only shift  $K_1$  and  $K_3$  differentially, but also  $K_5$  and/or  $K_6$ . An apparent anomaly is the opposite effect of  $K^+$  on  $P_i$  and vanadate binding:  $K^+$  increases the  $K_i$  for  $P_i$  (Table II) but decreases the  $K_d$  for vanadate [25]. If vanadate binds as a transition state analog of  $P_i$  leaving  $E_2K$ -P [25], then this enzyme conformation would differ from that binding  $P_i$  and substrate, as expected.

## Acknowledgements

We wish to thank Drs. Philip Dunham and Robert Mercer for advice as well as providing the red blood cell preparations, and Dr. Marcia Steinberg for helpful discussions. This work was supported by U. S. Public Health Service Research grant NS-05430.

## References

- 1 Robinson, J.D. and Flashner, M.S. (1979) *Biochim. Biophys. Acta* 549, 145–176
- 2 Cantley, L.C. (1981) *Curr. Topics Bioenerg.* 11, 201–237
- 3 Schuurmans Stekhoven, F. and Bonting, S.L. (1981) *Physiol. Rev.* 61, 1–76
- 4 Albers, R.W. (1967) *Annu. Rev. Biochem.* 36, 727–756
- 5 Post, R.L., Kume, T., Tobin, T., Orcutt, B. and Sen, A.K. (1969) *J. Gen. Physiol.* 54, 306–326S
- 6 Karlsh, S.J.D. and Yates, D.W. (1978) *Biochim. Biophys. Acta* 527, 115–130
- 7 Jørgensen, P.L. (1975) *Biochim. Biophys. Acta* 401, 399–415
- 8 Robinson, J.D. (1982) *J. Bioenerg. Biomembranes* 14, 319–333
- 9 Karlsh, S.J.D., Yates, D.W. and Glynn, I.M. (1978) *Biochim. Biophys. Acta* 525, 252–264
- 10 Jørgensen, P.L. and Karlsh, S.J.D. (1980) *Biochim. Biophys. Acta* 597, 305–317
- 11 Robinson, J.D. (1967) *Biochemistry* 6, 3250–3258
- 12 Jørgensen, P.L. (1974) *Biochim. Biophys. Acta* 356, 36–52
- 13 Mercer, R.W. and Dunham, P.B. (1981) *J. Gen. Physiol.* 78, 547–568
- 14 Robinson, J.D. and Mercer, R.W. (1981) *J. Bioenerg. Biomembranes* 13, 205–218
- 15 Robinson, J.D. (1969) *Biochemistry* 8, 3348–3355
- 16 Robinson, J.D. (1972) *Biochim. Biophys. Acta* 274, 542–550
- 17 Robinson, J.D. (1970) *Arch. Biochem. Biophys.* 139, 164–171
- 18 Robinson, J.D. (1973) *Biochim. Biophys. Acta* 321, 662–670
- 19 Robinson, J.D. (1981) *Biochim. Biophys. Acta* 645, 405–417
- 20 Robinson, J.D. (1970) *Biochim. Biophys. Acta* 212, 509–511
- 21 Cornish-Bowden, A. (1979) *Fundamentals of Enzyme Kinetics*, p. 61, Butterworths, London
- 22 Skou, J.C. and Esmann, M. (1980) *Biochim. Biophys. Acta* 601, 386–402
- 23 Jørgensen, P.L. and Petersen, J. (1982) *Biochim. Biophys. Acta* 705, 38–47
- 24 Matsui, H. and Homareda, H. (1982) *J. Biochem.* 92, 193–217
- 25 Cantley, L.C., Jr., Cantley, L.G. and Josephson, L. (1978) *J. Biol. Chem.* 253, 7361–7368
- 26 Albers, R.W. and Koval, G.J. (1972) *J. Biol. Chem.* 247, 3088–3092
- 27 Robinson, J.D. (1971) *Biochem. Biophys. Res. Commun.* 42, 880–885
- 28 Drapeau, P. and Blostein, R. (1980) *J. Biol. Chem.* 255, 7827–7834
- 29 Albers, R.W. and Koval, G.J. (1973) *J. Biol. Chem.* 248, 777–784
- 30 Robinson, J.D. (1977) *Biochim. Biophys. Acta* 482, 427–437
- 31 Robinson, J.D. (1983) *Curr. Topics Membrane Transp.*, in the press